

M-HOF-Opt: Multi-Objective Hierarchical Output Feedback Optimization via Multiplier Induced Loss Landscape Scheduling

Xudong Sun^{* 1} Nutan Chen² Alexej Gossmann³ Yu Xing⁴ Carla Feistner¹
 Emilio Dorigatti¹ Felix Drost¹ Daniele Scarcella¹ Lisa Beer¹ Carsten Marr¹

¹Institute of AI for Health, Computational Health Center, Helmholtz Munich, Munich, Germany

²Machine Learning Research Lab, Volkswagen Group, Munich, Germany

³U.S. FDA Center for Devices and Radiological Health, Silver Spring, MD, USA

⁴KTH Royal Institute of Technology, Stockholm, Sweden

Abstract

We address the online combinatorial choice of weight multipliers for multi-objective optimization of many loss terms parameterized by neural networks via a probabilistic graphical model (PGM) for the joint model parameter and multiplier evolution process, with a hypervolume based likelihood promoting multi-objective descent. The corresponding parameter and multiplier estimation as a sequential decision process is then cast into an optimal control problem, where the multi-objective descent goal is dispatched hierarchically into a series of constraint optimization sub-problems. The subproblem constraint automatically adapts itself according to Pareto dominance and serves as the setpoint for the low level multiplier controller to schedule loss landscapes via output feedback of each loss term. Our method is multiplier-free and operates at the timescale of epochs, thus saves tremendous computational resources compared to full training cycle multiplier tuning. It also circumvents the excessive memory requirements and heavy computational burden of existing multi-objective deep learning methods. We applied it to domain invariant variational auto-encoding with 6 loss terms on the PACS domain generalization task, and observed robust performance across a range of controller hyperparameters, as well as different multiplier initial conditions, outperforming other multiplier scheduling methods. We offered modular implementation of our method, admitting extension to custom definition of many loss terms.

1 INTRODUCTION

In many deep learning fields including domain generalization [Gulrajani and Lopez-Paz, 2020], the loss function for neural networks amounts to a summation of multiple terms, with a multiplier weighting each term. As the number of loss terms increases, the space of choice for those multipliers grows dramatically. In addition, when the validation set is drawn from a different distribution than the target domain, the validation performance does not faithfully reflect the target domain performance [Chen et al., 2022b] and can easily reach and maintain a saturated value during training. All these factors complicate and add difficulties to the process of model selection using conventional hyperparameter tuning [Probst et al., 2019] methods.

Instead of optimizing a fixed weighted summation of many neural network loss terms using a single objective optimization algorithm which relies on heavy hyperparameter tuning of the weight multipliers, multi-objective optimization on these loss terms has raised attention in the deep learning community recently [Sener and Koltun, 2018, Lin et al., 2019, Mahapatra and Rajan, 2021, Chen et al., 2022b]. Previous works in this direction [Mahapatra and Rajan, 2021, Chen et al., 2022b] addresses the problem via careful choice of multipliers at each optimization iteration instead of fixed for the whole training cycle, but suffers from excessive memory requirement and heavy extra computation burden, which hinders their applicability to large dataset and large scale neural networks Chen et al. [2022b]. Furthermore, it is restricted to **Exact** Pareto optimization [Mahapatra and Rajan, 2021] where the solution should be aligned to a user input preference vector, while how to set that is not clear in the general case. Their performance further relies on careful tuning of learning rate of single objective low level optimization algorithms Chen et al. [2022b]. Single objective optimization algorithms like ADAM [Kingma and Ba,

* ac.xudong.sun@gmail.com

code: <https://github.com/marrlab/DomainLab/tree/mhof>

2015] were analyzed predominantly with convex optimization theory [Kingma and Ba, 2015, Reddi et al., 2019], which does not hold globally [Milne, 2019]. From a control theory point of view, these low level optimization algorithms drive the model parameters iteratively, which forms a dynamic system. Due to lack of comprehensive theoretical underpinnings of the loss function property with respect to model parameters, this dynamic system has unreliable open-loop behavior.

Inspired by feedback control theory [Doyle et al., 2013] and feedback optimization in power systems [Piccallo et al., 2020, He et al., 2023, Hauswirth et al., 2024], we treat the dynamic system of model parameters driven by the low level optimization algorithm as an uncontrolled plant, with model parameter as state and the many loss terms as output. We use state dependent multiplier induced loss landscapes as control input and designed a hierarchical control structure [Dietterich et al., 1998, Kulkarni et al., 2016, Sun et al., 2020] to drive the system towards a multi-objective descent goal, without modifying the internal dynamic of low level neural network optimization algorithms.

This hierarchical control structure allows for a more refined and flexible approach to high-level optimization of neural networks, by automatically balancing the trade-off between a task-specific empirical loss and various regularization losses, which we detail in Equation (1). We depicted our idea in the control diagram in Figure 1 where the motivation of choosing multiplier induced landscape scheduling as control input is illustrated in Figure 4.

We demonstrated that our method removes the combination curse of dimensionality of multi-dimensional multipliers, via training domain invariant variational auto-encoding [Ilse et al., 2020] on the PACS dataset. Our method only has a small number of hyperparameters for our controllers while achieving robust performance when changing them. The baselines include different warmup multiplier scheduling strategies, which still need explicit specification of multiplier ultimate values. Their performance varies drastically with changes in those ultimate values. We attribute the improved performance of our method to the automatic trade-off of different loss terms. Our major contributions are:

- We proposed a probabilistic graphical model (PGM) for depicting the joint multiplier and model parameter adaptation process with a likelihood function imposed, promoting multi-objective descent of each loss term, which can be used to described general multi-objective deep learning. We proposed to transform the problem of parameter inference of this PGM into a sequen-

tial decision process through an optimal control formulation.

- We proposed to solve the sequential decision process for the multi-objective descent goal via breaking the goal into a series of constraint optimization sub-goals which forms a hierarchical controller that automatically adjusts the value of both the multiplier and the model parameters during the training process. The constraint bound updates itself via Pareto dominance. The multi-objective descent of the empirical risk and multi-dimensional penalty (regularization) loss in Equation (1) offers additional model selection criteria along with validation set performance. Compared to Bayesian optimization, our controller operates at the timescale of model parameter dynamic epoch instead of a complete training, which saves tremendous computational resources. Compared to existing multi-objective deep learning methods, it circumvent excessive memory requirements and heavy extra computational burden.
- When treating the neural network model parameter dynamic system driven by low level optimization algorithm as uncontrolled plant, we proposed to use state dependent multiplier induced loss landscapes as control input (see Figure 4) and offered initial theoretical analysis of the multi-objective descent behavior of our closed loop system. We offered modular implementation of our method ¹ and showed robustness of our method with respect to different multiplier initial conditions and controller hyperparameters for domain generalization on the PACS dataset with domain invariant auto-encoding.

2 PRELIMINARIES

2.1 STRUCTURAL RISK MINIMIZATION

Structural Risk Minimization (SRM) is a principle in learning algorithms that balances training performance and model complexity via optimizing the penalized loss in Equation (1).

$$L(\theta, \mu, \mathcal{D}_{tr}) = \ell(\theta, \mathcal{D}_{tr}) + \mu^T R(\theta, \mathcal{D}_{tr}) \quad (1)$$

$$\mu, R(\cdot) \in \mathbb{R}_+^d$$

In Equation (1), we consider loss L with training data \mathcal{D}_{tr} and model parameters θ . $\ell(\theta, \mathcal{D}_{tr})$ represents the empirical risk and $R(\theta, \mathcal{D}_{tr})$ represents the regularization term of the loss function, also referred to as the penalty function and thus L the penalized loss. \mathbb{R}_+^d is the d dimensional positive octant. We refer to the

¹<https://github.com/marrlab/DomainLab/tree/mhof>

multiplier μ as the penalty multiplier, as a special case of general hyperparameters (e.g. learning rate) in deep learning.

Notation In the following sections, for brevity, we omit the implicit dependence of $\ell(\cdot)$ and $R(\cdot)$ on \mathcal{D}_{tr} and θ . We also write $R(\theta, \cdot)$ where we need an explicit dependence on θ but use \cdot only to represent data \mathcal{D}_{tr} and/or other arguments. We use subscript of $R(\cdot)$ to indicate the component of $R(\cdot)$ corresponding to that subscript, e.g., if $\mu = [\beta, \gamma]$, then $R_\beta(\cdot)$ corresponds to the component of $R(\cdot)$ associated with β . We use $X, Y \sim \mathcal{D}$ to represent a random variable X and its supervision signal Y from distribution \mathcal{D} and we use the same symbol \mathcal{D} to denote a corresponding dataset as well. Let x be an instance of X , so is y for Y .

We use superscript k in bracket to index the optimization iteration, which by default corresponds to one epoch for our method (it can also correspond to one training cycle in Equation (2) to iteratively achieve Equation (3) for conventional hyperparameter optimization, see Remark 3.1).

Definition 2.1. When optimizing Equation (1) with multiplier μ iteratively (e.g. with gradient based methods like ADAM), the model parameter evolution dynamic $\theta^{(k+1)} = f_\theta(\mu, \theta^{(k)}, \mathcal{D}_{tr})$ brings $\theta^{(k)}$ to its next value $\theta^{(k+1)}$. $\theta^{(k+1)}$ then becomes the initial value for further iterations. For notational simplicity, we replace the explicit dependence of this dynamic on training data \mathcal{D}_{tr} , multiplier μ (potentially varying value for each iteration) and/or even the initial model parameter θ with dots. This convention results in notations $f_\theta(\theta, \cdot)$, $f_\theta(\mu, \cdot)$ and $f_\theta(\cdot)$. We also write $\theta^+ = f_\theta(\mu, \theta, \cdot)$ and $\theta^+ = f_\theta(\theta, \cdot)$ (potentially varying μ for each iteration) to represent the model parameter dynamic system without explicitly using k .

2.2 MULTI-OBJECTIVE OPTIMIZATION

Definition 2.2. We use $R(\theta_1, \cdot) \prec R(\theta_2, \cdot)$ (see Equation (1)) to indicate each component of the d dimensional vector $R(\theta_1, \cdot)$ is \leq the corresponding component of $R(\theta_2, \cdot)$. We use $\not\prec$ as the negation of \prec . The clause $\ell(\theta_1, \cdot), R(\theta_1, \cdot) \not\prec \ell(\theta_2, \cdot), R(\theta_2, \cdot)$ AND $\ell(\theta_2, \cdot), R(\theta_2, \cdot) \not\prec \ell(\theta_1, \cdot), R(\theta_1, \cdot)$ defines an equivalence relation which we denote as $\theta_1 \sim \theta_2$.

Definition 2.3. Starting from $\theta^{(0)}$, under dynamic system $\theta^+ = f_\theta(\theta, \cdot)$, we use $s\mathcal{R}(\theta^{(0)}, f_\theta(\cdot))$ to represent the set of model parameters (θ points) that can be reached. Accordingly, we use $v\mathcal{R}_{\ell(\cdot), R(\cdot)}(\theta^{(0)}, f_\theta(\cdot))$ to represent the corresponding set of multi-objective function values.

Definition 2.4. If $\theta_1 \sim \theta_2$ where $\theta_1 \in s\mathcal{R}(\theta^{(0)}, f_\theta(\cdot))$ and $\theta_2 \in s\mathcal{R}(\theta^{(0)}, f_\theta(\cdot))$ as in Definition 2.3, we define $\theta_2 \in \mathcal{C}_{\ell(\cdot), R(\cdot)}(\theta_1, f_\theta(\cdot), \theta^{(0)})$ the map from a representing element θ_1 to its equivalence class, which contains θ_2 . We use $\mathcal{E}_{\ell(\cdot), R(\cdot)}(\theta_1, f_\theta(\cdot), \theta^{(0)})$ to represent the set of $\ell(\cdot), R(\cdot)$ values for each element of $\mathcal{C}_{\ell(\cdot), R(\cdot)}(\theta_1, f_\theta(\cdot), \theta^{(0)})$.

2.3 HYPERPARAMETER TUNING

The multiplier μ in Equation (1) is a hyperparameter that affects the evolution of the model parameters θ in the optimization process for L defined in Equation (1), which leads to optimized model parameter $\theta_{\mu, \mathcal{D}_{tr}}$ below, where we omit the potential dependence of $\theta_{\mu, \mathcal{D}_{tr}}$ on its initial condition $\theta^{(0)}$ for notational simplicity.

$$\theta_{\mu, \mathcal{D}_{tr}} = \arg \min_{\theta} L(\theta, \mu, \mathcal{D}_{tr}). \quad (2)$$

Hyperparameter optimization aims to adjust the multiplier μ in alignment with specific performance metrics O (e.g. validation set accuracy for a classification task) in Equation (3) evaluated on the validation set \mathcal{D}_{val} , which lead to the selected hyperparameter $\mu_{\mathcal{D}_{tr}, \mathcal{D}_{val}}$.

$$\mu_{\mathcal{D}_{tr}, \mathcal{D}_{val}} = \arg \min_{\mu} O(\theta_{\mu, \mathcal{D}_{tr}}, \mathcal{D}_{val}). \quad (3)$$

The process of hyperparameter optimization in Equation (3) leads to selected model $\theta_{\mu_{\mathcal{D}_{tr}, \mathcal{D}_{val}}, \mathcal{D}_{tr}}$, which can be conceptualized as a problem of algorithm configuration [Hutter et al., 2007, 2014, López-Ibáñez et al., 2016, Sun et al., 2020] where the hyperparameter configures a machine learning algorithm.

To solve Equation (3) iteratively, each iteration relies on a complete training cycle to optimize Equation (2). The selection of μ depends on validation set \mathcal{D}_{val} , which can only be drawn from a different distribution compared to the target domain for the domain generalization problem (Section 2.4). Additionally, the performance metric O on the in-domain validation set can reach and maintain a saturated value during training with neural networks of high expressive power.

2.4 DOMAIN GENERALIZATION

Domain generalization aims at enabling the trained neural network to achieve robust generalization to unseen domains exhibiting distribution shifts [Gulrajani and Lopez-Paz, 2020, Sun et al., 2019b]. Many domain generalization methods [Ganin et al., 2016, Li et al., 2018, Levi et al., 2021, Carlucci et al., 2019, Ilse et al.,

2020, Sun and Buettner, 2021, Rame et al., 2022] promotes this goal via domain invariant representation by adding domain invariant regularization losses $R(\cdot)$ upon task-specific losses $\ell(\cdot)$ (e.g. classification loss) on the training data in Equation (1).

As an example of $\ell(\cdot) + \mu^T R(\cdot)$ loss for domain generalization, we label each component of the loss of Domain Invariant Variational Autoencoding (DIVA) [Ilse et al., 2020] in the following equations, where we use x to denote the input instance (e.g. input image), y to denote the corresponding supervision class label, and d the domain label. DIVA [Ilse et al., 2020] aims to disentangle domain specific information with learned features z_d and class specific information with z_y , and has two corresponding classification losses $\mathbb{E}_{q_{\phi_y}(z_y|x)}[\log q_{\omega_y}(y|z_y)]$ (classifying the correct class label based on z_y) and $\mathbb{E}_{q_{\phi_d}(z_d|x)}[\log q_{\omega_d}(d|z_d)]$ (classifying the correct domain label based on z_d).

$$L(\theta, \mu, x, y, d) = \ell(\cdot) + \mu^T R(\cdot) = \quad (4)$$

$$\gamma_y \mathbb{E}_{q_{\phi_y}(z_y|x)}[\log q_{\omega_y}(y|z_y)] + \quad (5)$$

$$\mu_{recon} \mathbb{E}_{q_{\phi_d}(z_d|x), q(z_x|x), q(z_y|x)} \log p_{\theta_r}(x|z_d, z_x, z_y) + \quad (6)$$

$$[-\beta_x KL(q_{\phi_x}(z_x|x)||p_{\theta_x}(z_x))] + \quad (7)$$

$$[-\beta_y KL(q_{\phi_y}(z_y|x)||p_{\theta_y}(z_y|y))] + \quad (8)$$

$$[-\beta_d KL(q_{\phi_d}(z_d|x)||p_{\theta_d}(z_d|d))] + \quad (9)$$

$$\gamma_d \mathbb{E}_{q_{\phi_d}(z_d|x)}[\log q_{\omega_d}(d|z_d)] \quad (10)$$

Here, KL denotes Kullback-Leibler divergence, \mathbb{E} denotes expectation, $p(\cdot)$ stands for the prior distribution or the distribution of the generative model, and $q(\cdot)$ stands for the approximate posterior distribution. For more details, refer to [Ilse et al., 2020]. In the above situation, we have $\mu = [\mu_{recon}, \beta_x, \beta_y, \beta_d, \gamma_d]$ and $\theta = [\phi_x, \phi_d, \theta_r, \theta_d, \theta_x, \theta_y, \phi_x, \phi_y, \phi_d, \omega_d, \omega_y]$ with each entry representing the weight (with bias) of a neural network.

In [Ilse et al., 2020], $\mu_{recon} = 1.0$ in Equation (6). Additionally, γ_y and γ_d are maintained as constants. γ_y is corresponding to $\ell(\cdot) = \gamma_y \mathbb{E}_{q_{\phi_y}(z_y|x)}[\log q_{\omega_y}(y|z_y)]$ in Equation (5), and γ_d in Equation (10) is associated with one component of $R(\cdot)$. However, the combined choice of γ_y and γ_d significantly influences the generalization performance, as shown by our experimental findings in Section 5.

For the multiplier $\beta_x, \beta_y, \beta_d$ corresponding to other components of $R(\cdot)$, Ilse et al. [2020] used a warm-up strategy to increase them gradually from a small value to a pre-defined value. This, however, still requires a choice of the ultimate values for $\beta_x, \beta_y, \beta_d$. In [Ilse et al., 2020], these ultimate values are simply set to one. We coin this kind of multiplier scheduling

strategy a *feedforward* scheme. Note that this strategy does not reduce the number of hyperparameters to be selected, since ultimate values for the multipliers still have to be specified.

3 METHODS

In this section, we elaborate on the hierarchical output feedback control strategy for the multidimensional multiplier adaptation in Equation (1) (see Figure 1) towards multi-objective optimization. We propose a Probabilistic Graphical Model (PGM) for the joint model parameter and multiplier adaptation process in Section 3.1, which leads to an optimal control formulation of parameter estimation, extending the classical hyperparameter tuning-based approach to parameter-multiplier co-evolution in Section 3.2.

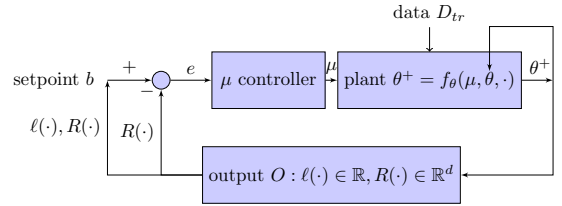


Figure 1: A control diagram illustrating the hierarchical output feedback optimization process we proposed with multi-objective setpoint adaptation. The uncontrolled plant corresponds to an open loop dynamic $\theta^+ = f_{\theta}(\mu, \theta, \cdot)$ via optimizing Equation (1) with a low level optimization algorithm (e.g. ADAM) lacking feedback. The μ controller adjusts the multiplier μ , thus schedules loss landscape (see Illustration in Figure 4), based on the difference e between the setpoint b (defined in Equation (23)) and the measured output components $R(\cdot)$, guiding the optimization of model parameters θ through a feedback loop. The setpoint b is adjusted via feedback from $\ell(\cdot)$ and $R(\cdot)$ (Equation (24a)) which forms a higher hierarchy.

3.1 PROBABILISTIC GRAPHICAL MODEL FOR PARAMETER AND MULTIPLIER ADAPTIVE OPTIMIZATION PROCESS

Gradient based optimization algorithms for neural network defines a dynamic system for model parameters where the weight multiplier in Equation (1) configures such a dynamic system. Instead of using fixed multipliers (or fixed multipliers' ultimate values), we propose to choose the multiplier values also dynamically. Due to the stochastic nature of the gradient based optimization process in deep learning with different subsam-

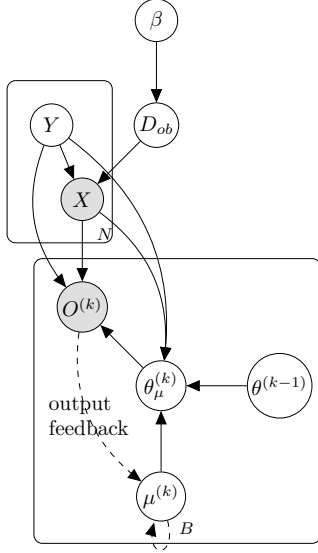


Figure 2: A probabilistic graphical model for the sequential decision process of joint multiplier and model parameter adaptation in multiple-domain (data-site specific distribution) supervised learning.

ple and mini-batch distributions for each iteration, it is appropriate to use a Probabilistic Graphical Model (PGM) to describe such a stochastic process. PGM has been used to describe sequential decision processes like reinforcement learning [Levine, 2018, Sun and Bischl, 2019]. We propose Figure 2 to describe the sequential decision process of model parameter and multiplier adaptation in the form of a probabilistic graphical model (PGM) [Koller and Friedman, 2009]. In the upper part of Figure 2, we model the generative process of N observations of the instance X (e.g. an image) and the corresponding supervision signal Y (e.g. a class label). The path $\beta \rightarrow D_{ob} \rightarrow X$, where, D_{ob} is the path $\beta \rightarrow D_{ob} \rightarrow X$, where, D_{ob} is the data-site Sun et al. [2019a] specific prior parameter (domain variable, characterizing distribution) with hyper-prior β , models the information which is not captured by the supervision signal Y of X .

In the lower part of the graphical model, with superscript k representing the iteration for the decision process, we use $\mu^{(k)}$ to represent the multiplier of the loss in Equation (1) at the k th iteration. The multiplier $\mu^{(k)}$ serves as a configuration parameter for the optimization process of Equation (1) that affects the value of $\theta_{\mu}^{(k)}$, evolved from its previous value $\theta^{(k-1)}$. $\theta_{\mu}^{(k)}$ then becomes the initial value for the next iteration. This can be described in Equation (14) with explicit dependence of $\theta^{(k)}$ on $\mu^{(k)}$ omitted. The model parameter $\theta^{(k)}$ and observed data X , supervision signal Y co-parent the performance indicator as output $O^{(k)}$.

The plate replicates B in the lower part represents the

number of optimization iterations (each iteration correspond to N observations). The adaptive generation of the next multiplier $\mu^{(k+1)}$ depends on the previous value $\mu^{(k)}$ (the self-loop dashed arrow in Figure 2) and the feedback information of the output $O^{(k)}$ (long dashed arrow), as in Equation (11).

$$\mu^{(k+1)} = f_{\mu}(\mu^{(k)}, O^{(k)}, \cdot) \quad (11)$$

Remark 3.1. An example of f_{μ} can be based on the acquisition function in Bayesian optimization (BO) [Garnett, 2023] for approximating Equation (3), which leads to a BO realization of this PGM in [Sun et al., 2019a], where O in Equation (11) is usually chosen to be the validation set prediction performance and iteration index k corresponds to a whole training cycle of Equation (2) to iteratively achieve Equation (3).

Different from the BO realization of this PGM, which generates multipliers at a much slower timescale (usually once at the end of training) than that for the evolution of model parameters in neural network training, the hierarchical output feedback optimization we proposed (Figure 1 and elaborated in following sections) operates at the timescale of epoch, thus forms another realization of this PGM with iteration index k corresponding to epochs. In addition, we have $O(\cdot) = \ell(\cdot), R(\cdot)$ for the PGM in Figure 2 in contrast to validation set performance used in BO.

We introduce an objective function for estimating $\theta_{\mu^{(B)}}$ based on the profile likelihood in eq. (12) in accordance with the PGM in Figure 2. This likelihood promotes a high $e\mathcal{H}\mathcal{V}(\cdot)$ in Definition 3.1 with respect to $\theta_{\mu^{(B)}}$. Ξ is the normalization factor.

$$\mathcal{P}(\theta_{\mu^{(B)}}) = \frac{1}{\Xi} \exp \left(e\mathcal{H}\mathcal{V}_{O(\cdot)=\ell(\cdot), R(\cdot)}(\theta_{\mu^{(B)}}, \theta^{(0)}, f_{\theta}, \cdot) \right) \quad (12)$$

Definition 3.1. $e\mathcal{H}\mathcal{V}_{O(\cdot)=\ell(\cdot), R(\cdot)}(\theta, \theta^{(0)}, f_{\theta}, \cdot)$ maps θ to the dominated hypervolume [Zitzler and Künzli, 2004, Zitzler et al., 2007, Guerreiro et al., 2021] of $\mathcal{E}_{\ell(\cdot), R(\cdot)}(\theta, f_{\theta}(\cdot), \theta^{(0)})$ in Definition 2.4 with respect to reference point $\ell(\theta^{(0)}, \cdot) \in \mathbb{R}, R(\theta^{(0)}, \cdot) \in \mathbb{R}^d$. As illustrated in Figure 3.

The PGM we defined here can also be used to describe other multi-objective deep learning methods Mahapatra and Rajan [2021] via online combinatorial choice of multipliers.

Remark 3.2. The PGM also provides a potential possibility to impose a Bayesian interpretation to the joint multiplier tuning and model training process for frequentist machine learning models, the deeper investigation of which we leave for future work.

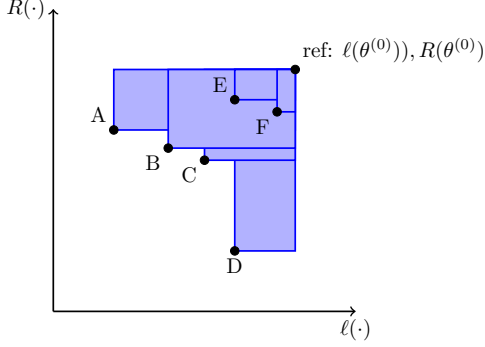


Figure 3: Illustration to $e\mathcal{HV}$ in Definition 3.1: We take $[\ell(\theta^{(0)}, \cdot) \in \mathbb{R}, R(\theta^{(0)}) \in \mathbb{R}^{d=1}]$ as reference point. Suppose $\{A, B, C, D, E, F\}$ in the illustration constitute $v\mathcal{R}(\theta^{(0)}, f_\theta(\cdot))$ in Definition 2.3. For any θ corresponding to the point A in the illustration with coordinate $[\ell(\theta, \cdot), R(\theta, \cdot)]$, $e\mathcal{HV}$ maps θ to $\mathcal{C}_{\ell(\cdot), R(\cdot)}(\theta, f_\theta(\cdot), \theta^{(0)})$, then to $\mathcal{E}_{\ell(\cdot), R(\cdot)}(\theta, f_\theta(\cdot), \theta^{(0)})$ (see Definition 2.4), which is the point set $\{A, B, C, D\}$, then it calculates the dominated hypervolume with respect to the reference point (union of the shaded rectangles).

3.2 HIERARCHICAL CONTROL FORMULATION OF JOINT PARAMETER MULTIPLIER OPTIMIZATION

3.2.1 Optimal control formulation

Analogous to how optimal control Lewis et al. [2012] can be formulated as maximum likelihood estimation in a probabilistic graphical model [Levine, 2018, Sun and Bischl, 2019], the estimation of $\theta^{(B)}$ based on the profile likelihood like objective in Equation (12) for Figure 2 is also a sequential decision process. From a statistical inference point of view, we are conducting a sequential inference (i.e., finding a sequence of μ in Equation (13)), such that the last step B has the best possible hyper-volume with respect to output O (in a stochastic sense, see Figure 3), where O can be a performance metric like accuracy on the validation set in Bayesian optimization, or defined in Equation (15) for our method.

To reformulate the estimation problem as an optimal control problem, we present the sequential decision on choosing a sequence of multipliers $\mu^{(1)}, \dots, \mu^{(B)}$ defined in Equation (1) with respect to the objective function in Equation (13) at iteration B which pro-

motes Equation (12).

$$\min_{\mu^{(1)}, \dots, \mu^{(k)}, \dots, \mu^{(B)}} e\mathcal{HV}_{O(\cdot)}(\theta_{\mu^{(B)}}, \theta^{(0)}, f_\theta, \cdot) \quad (13)$$

$$\text{s.t. } \theta^{(k)} = f_\theta(\mu^{(k)}, \theta^{(k-1)}, \cdot) \quad (14)$$

$$O^{(k)} = [\ell(\theta^{(k)}|\cdot), R(\theta^{(k)}|\cdot)] \quad (15)$$

$$k = 0, 1, \dots, B \quad (16)$$

Here, we use θ to denote the neural network weights, which can be regarded as the state of a dynamic system, where the state transition is governed by a low level model parameter optimization dynamic f_θ in Equation (14) (e.g. ADAM [Kingma and Ba, 2015]). From a control theory point of view, f_θ depicts the uncertain dynamic of a plant to be controlled, while the task here is to define a controller to generate a μ sequence to guide the uncertain dynamic of θ with respect to plant output O , as depicted in Figure 1. We treat the loss terms $R(\cdot)$ and $\ell(\cdot)$ as the output of the system in Equation (15). From a statistical point of view, f_θ corresponds to the parent structure of $\theta^{(k)}$ in Figure 2, which drives θ to the next value.

Although we have no complete knowledge of f_θ from Equation (14) describing low level optimization algorithms like ADAM, in practice, the penalized loss from Equation (1) often descent after some number of iterations (possibly with oscillations in between), which leads to Definition 3.2.

Definition 3.2. A penalized loss descent operator \mathcal{G} satisfies that if $\theta^+ \in \mathcal{G}_\mu(\theta; \ell(\cdot), R(\cdot))$, then $\ell(\theta^+) + \mu R(\theta^+) < \ell(\theta) + \mu R(\theta)$

Therefore, we take the frequent occurrences of operators in Definition 3.2 during neural network training as a mild assumption in our following discussion. For instance, we could run f_θ in Equation (14) in one step to have $\ell(\theta^{(k+1)}) + \mu^{(k+1)} R(\theta^{(k+1)}) < \ell(\theta^{(k)}) + \mu R(\theta^{(k)})$, or in more than one steps to achieve Definition 3.2.

Our final goal, however, is to ensure a joint descent of $\ell(\cdot)$ and $R(\cdot)$, which leads to Definition 3.3:

Definition 3.3. A Pareto-descent operator takes θ to $\theta^{(+)}$ (via one or several iterations) which descents $R(\cdot)$ and $\ell(\cdot)$ simultaneously, i.e.,

$$\ell(\theta^+) < \ell(\theta) \quad (17)$$

$$R(\theta^+) \preceq R(\theta) \quad (18)$$

3.2.2 Multi-objective optimization via shrinking the reference signal in constrained optimization

A concrete form of Equation (11) will detail how μ is updated by a controller f_μ . Combining Equations (11)

and (14), we have

$$\theta^{(k+1)} = f_\theta(f_\mu(\mu^{(k)}, O^{(k)}), \theta^{(k)}, \cdot) \quad (19)$$

$$= f_{\theta, \mu}^k(\mu^{(0)}, \theta^{(0)}, \cdot) \quad (20)$$

where we use $f_{\theta, \mu}^k$ to represent the k -times compound recursive evaluations of f_θ and f_μ in Equation (19) until the dependence is only on $\theta^{(0)}, \mu^{(0)}$. We call Equation (20) the *closed-loop* dynamics for θ .

The question then arises: how can we design such a closed-loop dynamic system to ensure a Pareto descent of $O(\cdot)$ (both $R(\cdot)$ and $\ell(\cdot)$), leading to multi-objective optimization in Definition 3.3 or Equation (13)?

To resolve this, we reduce it to a simpler problem, i.e., when bounding the regularization term $R(\cdot)$ from above by a time-varying reference $b^{(k)}$ (a.k.a. set-point) in eq. (26), what value can we achieve for $\ell(\cdot)$ at Equation (25). If we could ensure the bound changes monotonically, multi-objective optimization can be achieved.

First, we define the time-varying reference signal being governed by the following:

$$b^{(0)} = \rho R^{(0)} \quad (21)$$

$$0 < \rho \in \mathbb{R} < 1 \quad (22)$$

$$b^{(k)} = g_b(\ell^{(0:k)}(\cdot), R^{(0:k)}(\cdot)) \quad (23)$$

where $g_b(\cdot)$ represents the mapping from the previous value at the training step $k-1$ to the new value at step k , defined as

$$b^{(k)} = \begin{cases} R^{(k)}, & \text{if } R^{(k)} < b^{(k-1)} \wedge \ell^{(k)} < \min_j \ell^{(j)} & (24a) \\ j = 0, \dots, k-1 & & (24b) \\ b^{(k-1)}, & \text{otherwise} & (24c) \end{cases}$$

Remark 3.3. Note that although $b^{(k)}$ is only defined for $R^{(k)}(\cdot)$, the shrinkage of $b^{(k)}$ also depends on $\ell(\cdot)$ decrease, thus indicates multi-objective Pareto-descent in Definition 3.3.

With $b^{(k)}$ defined above, under s_k iterations (number of iterations s_k depends on $\theta^{(k)}$), with $b^{(k)}$ fixed, i.e. $b^{(k)} = b^{(k+1)} = \dots = b^{(k+s_k-1)}$, suppose the following constrained optimization Bertsekas [2014] problem starting with $\theta^{(k)}$ has a solution and could be approximated:

$$\ell^{(k+s_k)}(\cdot) = \min_{\mu^{(k+1)}, \dots, \mu^{(k+s_k)}} \ell(\cdot) \quad (25)$$

$$\text{s.t. } R^{(k+s_k)}(\cdot) < b^{(k)} \quad (26)$$

$$R^{(j)}(\cdot) \not< b^{(k)} \quad (27)$$

$$\theta^{(j+1)} = f_\theta(\mu^{(j+1)}; \theta^{(j)}) \text{ (Equation (14))} \quad (28)$$

$$j = k, k+1, \dots, k+s_k-1 \quad (29)$$

Then, regardless if the minimization in Equation (25) is attainable or not, as long as we have

$$\ell^{(k+m)}(\cdot) < \ell^{(k)}(\cdot), \quad (30)$$

$$\exists m \geq s_k \quad (31)$$

, due to Equation (26), Equation (24a), we still achieve multi-objective decrease in Definition 3.3 at step $k+m$ compared to step k .

The evolution process of the model parameters in this case can be regarded as a plant with uncertain dynamic f_θ in Equations (14) and (28), where the only control we have at hand is the sequence $\mu^{(k+1)}, \dots, \mu^{(k+s_k)}$, which provides different loss landscapes at different iterations with different θ values as depicted in Figure 4. How can we design such μ or loss landscape sequence to promote Equation (26) to happen?

To simplify the discussion, first consider $\mu, R(\cdot) \in \mathbb{R}_+^{d=1}$. Before the constraint in Equation (26) is satisfied, design $\mu^{(k+1)}, \dots, \mu^{(k+s_k)}$ to be an increasing sequence Bazarraa et al. [2013], which gives more weight to the corresponding regularization term in $R(\cdot)$, to approximate the constraint optimization in Equation (25) by optimizing Equation (1) for each μ until Equation (26) is satisfied. However, will the increased weight on the regularization term in $R(\cdot)$ result in deteriorated $\ell(\cdot)$?

One possibility can be, although $f_\theta(\mu^{(k+1)}, \cdot)$ brings $\theta^{(k)}$ to the next value $\theta^{(k+1)}$ which decreases the penalized loss in Equation (1) with the new $\mu^{(k+1)}$, but the new $\theta^{(k+1)}$ evaluates to a deteriorated penalized loss with respect to the old $\mu^{(k)}$ as shown in Figure 4. To describe this behavior during the increasing process of μ , we have Equation (33) in Definition 3.4. This situation is of particular interest due to the possibility of overcoming local minima of a fixed loss landscape, as indicated in Figure 4.

Definition 3.4. A reg-Pareto slider $\mathcal{A}(\cdot)$ with respect to function $\ell(\cdot)$ and $R(\cdot)$ is defined to be a set map, s.t. if $\{\theta^{(k+1)}, \mu^{(k+1)}\} \in \mathcal{A}(\ell(\cdot), R(\cdot); \theta^{(k)}, \mu^{(k)})$ then

$$\ell(\theta^{(k+1)}) + \mu^{(k+1)} R(\theta^{(k+1)}) \leq \ell(\theta^{(k)}) + \mu^{(k+1)} R(\theta^{(k)}) \quad (32)$$

$$\ell(\theta^{(k+1)}) + \mu^{(k)} R(\theta^{(k+1)}) \geq \ell(\theta^{(k)}) + \mu^{(k)} R(\theta^{(k)}) \quad (33)$$

$$\mu^{(k+1)} \geq \mu^{(k)} \quad (34)$$

In this situation, take $R(\cdot) \in \mathbb{R}^{d=1}$, we have the following conclusion in Corollary 3.1 where we show the increase of $\ell(\cdot)$ as an expense to decrease of $R(\cdot)$ is bounded.

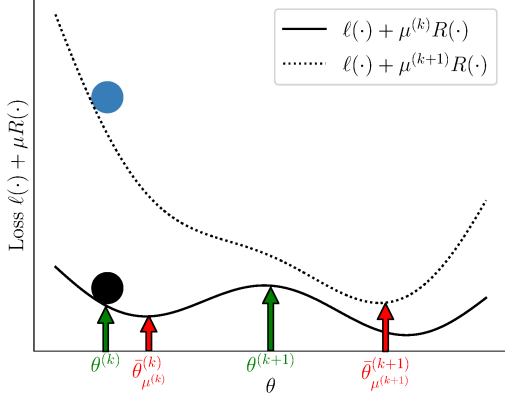


Figure 4: Illustration of the concept of multiplier induced loss landscape scheduling we proposed, used as control signal in Figure 1: The lifted landscape $\ell(\cdot) + \mu^{(k+1)}R(\cdot)$ (dotted curve) scheduled at iteration $k + 1$, enables the model parameter dynamic to overcome the local minimum $\theta_{\mu^{(k)}}^{(k)}$ of the old loss landscape $\ell(\cdot) + \mu^{(k)}R(\cdot)$ (solid curve) scheduled at iteration k , as can be imagined via the two balls with different colors rolling along the corresponding loss landscapes. It showcases a scenario corresponding to Definition 3.4: In comparison to $\theta^{(k)}$, $\theta^{(k+1)}$ corresponds to a decreased $\ell(\cdot) + \mu^{(k+1)}R(\cdot)$ value but increased $\ell(\cdot) + \mu^{(k)}R(\cdot)$ value.

Corollary 3.1. Let

$$\{\theta^{(k+1)}, \mu^{(k+1)}\} \in \mathcal{A}(\ell(\cdot), R(\cdot); \theta^{(k)}, \mu^{(k)}) \quad (35)$$

from definition 3.4 then,

$$R(\theta^{(k+1)}) \leq R(\theta^{(k)}) \quad (36)$$

$$\ell(\theta^{(k+1)}) \geq \ell(\theta^{(k)}) \quad (37)$$

$$\ell(\theta^{(k+1)}) - \ell(\theta^{(k)}) \leq \mu^{(k+1)}(R(\theta^{(k)}) - R(\theta^{(k+1)})) \quad (38)$$

Proof. Multiply -1 to both sides of Equation (33), add the results to Equation (32), we have

$$(\mu^{(k+1)} - \mu^{(k)})R(\theta^{(k+1)}) \leq (\mu^{(k+1)} - \mu^{(k)})R(\theta^{(k)}) \quad (39)$$

which implies

$$(\mu^{(k+1)} - \mu^{(k)}) \left(R(\theta^{(k+1)}) - R(\theta^{(k)}) \right) \leq 0 \quad (40)$$

Since $\mu^{(k+1)} > \mu^{(k)}$

$$R(\theta^{(k+1)}) - R(\theta^{(k)}) \leq 0 \quad (41)$$

Equation 33 and 32 give

$$0 \leq \mu^{(k)}(R(\theta^{(k)}) - R(\theta^{(k+1)})) \leq \quad (42)$$

$$\ell(\theta^{(k+1)}) - \ell(\theta^{(k)}) \leq \mu^{(k+1)}(R(\theta^{(k)}) - R(\theta^{(k+1)})) \quad (43)$$

□

Remark 3.4. In the case of $R(\cdot) \in \mathbb{R}^{d>1}$, when all components of μ increases, Equation (32) and Equation (33) imply at least one component of $R(\cdot)$ will decrease. We defer to Remark 3.6 and Section 3.2.3 for the discussion on when some components of μ increases while other components decreases.

Remark 3.5. Definition 3.4 and Corollary 3.1 gives a condition of decreasing $R(\cdot)$ at the expense of increasing $\ell(\cdot)$ (increase bounded though) at iteration k . When the gradient component from $\ell(\cdot)$ and $R(\cdot)$ agrees with each other at another iteration, we could expect both objectives to decrease as in Definition 3.3. It can also be the case at a particular iteration, $\ell(\cdot)$ decreases at the expense of $R(\cdot)$ increases.

What is left unclear, however, is after the accumulative effect of several iterations, if $\exists m$ to ensure Equation (30). To answer this, first, Corollary 3.2 gives a bound on the accumulative change of $\ell(\cdot)$ with $m = B$.

Corollary 3.2. Suppose that for all $k = 0, \dots, B - 1$

$$\ell(\theta^{(k+1)}) + \mu^{(k+1)}R(\theta^{(k+1)}) \leq \ell(\theta^{(k)}) + \mu^{(k+1)}R(\theta^{(k)})$$

and $\mu^{(k+1)} > \mu^{(k)}$. Then

$$\ell(\theta^{(B)}) \leq \ell(\theta^{(0)}) + S_{>} + S_{<}, \quad (44)$$

where

$$S_{>} = \sum_{k \in \mathcal{K}_{>}} \mu^{(k+1)}(R(\theta^{(k)}) - R(\theta^{(k+1)})),$$

$$S_{<} = \sum_{k \in \mathcal{K}_{<}} \mu^{(k)}(R(\theta^{(k)}) - R(\theta^{(k+1)})),$$

$$\mathcal{K}_{>} = \{k \in \{0, \dots, B - 1\} : \text{Equation (33) holds.}\},$$

$$\mathcal{K}_{<} = \{0, \dots, B - 1\} \setminus \mathcal{K}_{>}.$$

Proof. For $k \in \mathcal{K}_{>}$ (Equation (33) holds), from Corollary 3.1 we have that

$$\ell(\theta^{(k+1)}) - \ell(\theta^{(k)}) \leq \mu^{(k+1)}(R(\theta^{(k)}) - R(\theta^{(k+1)})).$$

For $k \in \mathcal{K}_{<}$, it holds that

$$\ell(\theta^{(k+1)}) + \mu^{(k)}R(\theta^{(k+1)}) < \ell(\theta^{(k)}) + \mu^{(k)}R(\theta^{(k)}),$$

implying

$$\ell(\theta^{(k+1)}) - \ell(\theta^{(k)}) < \mu^{(k)}(R(\theta^{(k)}) - R(\theta^{(k+1)})).$$

Decomposing

$$\begin{aligned} & \ell(\theta^{(B)}) - \ell(\theta^{(0)}) \\ &= \sum_{k=0}^{B-1} [\ell(\theta^{(k+1)}) - \ell(\theta^{(k)})] \\ &= \left(\sum_{k \in \mathcal{K}_>} + \sum_{k \in \mathcal{K}_<} \right) [\ell(\theta^{(k+1)}) - \ell(\theta^{(k)})] \end{aligned}$$

yields the conclusion. \square

Based on Corollary 3.2, we have the following conjecture to ensure Equation (30)

Conjecture 3.1. Further decompose $S_<$ from Corollary 3.2 into $S_<^-$ and $S_<^+$ via decomposing $\mathcal{K}_<$ in Corollary 3.2 into $\mathcal{K}_<^-$ and $\mathcal{K}_<^+$. Here $\mathcal{K}_<^-$ corresponds to the situations of $\ell(\cdot)$ descent with $S_<^- < 0$. And $\mathcal{K}_<^+$ corresponds to the $\ell(\cdot)$ ascent cases but upperbounded by $S_<^+ = \sum_{k \in \mathcal{K}_<^+} \mu^{(k)} (R(\theta^{(k)}) - R(\theta^{(k+1)}))$. Then \exists sequence $\{\mu^{(k)}\}$ s.t.

$$\ell(\theta^{(B)}) \leq \ell(\theta^{(0)}) + S_> + S_<^+ + S_<^- < 0 \quad (45)$$

Remark 3.6. In the case of $d > 1$, as long as a loss component of $R(\cdot)^{(k)}$, say $R_1^{(k)}(\cdot)$ is not bounded by its corresponding setpoint component $b_1^{(k)}(\cdot)$, we can still increase the value of the μ component $\mu_1^{(k)}$ to give more weight to the corresponding loss component, until the loss component in question decreases below the setpoint. However, an increased μ component $\mu_1^{(k)}$ corresponds to more weight on the gradient component corresponding to $R_1^{(k)}(\cdot)$, which makes it harder for other components of $R(\cdot)$ and $\ell(\cdot)$ to decrease. Therefore, instead of always increasing each component of μ , if one component of R has overshoot over the setpoint (i.e. constraint switched from being not satisfied to satisfied with respect to a particular loss component), we decrease the μ value to give the other components of μ and R more feasible space to adjust themselves.

Remark 3.7. We could extend the conjecture above to $\exists \mu$ sequence such that after B iterations, Pareto descent in Definition 3.3 could be achieved (equivalently, setpoint should shrink see Remark 3.3). We did observe such a Pareto descent behavior, defined in Definition 3.3 in our experiment for the $d > 1$ case of Equation (4), e.g. see Figure 5 and Figure 6.

3.2.3 Output feedback PI-like controller

How exactly should the μ sequence discussed above look like? With the adaptive law from Equation (23)

for setpoint b , we design the following controller for μ :

$$e^{(k)} = R(\cdot) - b^{(k)} \quad (46)$$

$$\delta_I^{(k+1)} = (1 - \xi_d) \delta_I^{(k)} + \xi_d e^{(k)} \quad (47)$$

$$\mu^{(k+1)} = \max(\mu^{(k)} \exp^{\max(K_I \delta_I^{(k+1)}, v_{sat})}, \mu_{clip}) \quad (48)$$

$$K_I > 0 \quad (49)$$

$$K_I \in \mathbb{R}^d \quad (50)$$

$$k = 0, 1, \dots, B \quad (51)$$

In Equation (46), we calculate how far the current output is away from the setpoint b , which gets passed through a moving average in Equation (47) with ξ_d being the coefficient of moving average in Equation (47) [Rezende and Viola, 2018]. μ is the output of the controller in Equation (48), K_I is the control gain for PI (proportional-integration) Johnson and Moradi [2005] like control, $K_I \delta_I^{(k+1)}$ is component wise multiplication, \exp and \max are computed component wise, v_{sat} is the exponential shoulder saturation, μ_{clip} is the upper bound for μ . Note that μ_{clip} determines the dynamic range of μ while v_{sat} determines an upper bound about how fast μ changes.

Remark 3.8. To avoid arbitrary choice of $K_I \in \mathbb{R}^d$, we use $\delta^{(0)} = R^{(0)} - b^{(0)}$ in Equation (47) where $b^{(0)} = \rho R^{(0)}$ (a percentage ρ). We divide by ηv_{sat} with $0 < \eta < 1$ to get the value for K_I so that the hyperparameter for our algorithm is $\rho, \eta \in \mathbb{R}$ instead of $K_I \in \mathbb{R}^d$.

The whole process is summarized in Algorithm 1 and Figure 1.

Algorithm 1 Multi-objective Hierarchical Output Feedback Optimization

- 1: **procedure** M-HOF-OPT($\mu^{(0)}, \theta^{(0)}, \rho, \cdot$)
 - 2: Initialize $\mu^{(0)}$, calculate $b^{(0)} = \rho R^{(0)}$
 - 3: Compute K_I based on Remark 3.8
 - 4: **while** budget B not reached **do**
 - 5: Update μ from controller in Equation (48)
 - 6: Update θ via running Equation (14) with the updated μ value
 - 7: Adapt setpoint according to Equation (23).
 - 8: **end while**
 - 9: **return** $\theta^{(B)}$ \triangleright
 - 10: **end procedure**
-

3.2.4 Multi-objective setpoint based model selection

In general, the feasibility in Equation (26) becomes more difficult to be met each time the setpoint b shrinks. After several setpoint shrinkages, the difficulty

of attaining the feasibility can lead to an oscillating behavior of $R(\cdot)$ around the setpoint with uncontrolled amplitude, as shown in Figure 5. To circumvent this behavior, the up-to-event best model is selected at the last setpoint shrinkage.

4 RELATED WORK AND DISCUSSION

Multipliers warmup [Sønderby et al., 2016, Ilse et al., 2020] or phase-in [Sicilia et al., 2023] requires ultimate multiplier values for each loss term, thus necessitates hyperparameter (ultimate multiplier values) optimization. Other works, such as [Rezende and Viola, 2018, Klushyn et al., 2019], has introduced constraint optimization by representing the weights of loss terms using Lagrange multipliers, designed to prevent over-regularisation of a single term within the loss function, which is extended to multiple loss terms in [Chen et al., 2022a]. In addition, Shao et al. [2020] (only deals with 2 loss terms), Chen et al. [2022a] proposed similar multiplier adaptation schemes as in Section 3.2.3 where the multiplier changes with a rate proportional to how the corresponding loss component distances from a constraint bound. However, their methods relied on a fixed constraint bound for each loss term and fixed proportionate gain for each loss term (defined to be K_I in Equation (48) in our work), necessitating a hyperparameter search, which is challenging when the number of terms in the loss increases. Moreover, for some regularizers, such as the ones based on KL divergence, it is challenging to estimate the constraint bound range. Specifically in the field of domain generalization, it is not obvious how to choose the constraint bound value and other hyperparameters due to the lack of observations from the target domain, where the validation set from the training domain can easily reach a saturated value due to the high expressive power of modern neural networks.

In comparison, we deal with many loss terms with multidimensional multipliers and introduced Equation (23) to progressively adapt the constraint bound and Remark 3.8 to choose the multidimensional controller gain value, thus avoid exhaustive hyperparameter search. In addition to the control theory formulation for multiplier adjustment, we also provided a Probabilistic Graphical Model interpretation in Section 3.1 and a landscape scheduling interpretation in Figure 4. Furthermore, we discussed our method under the multi-objective optimization scheme compared to single-objective consideration from other works.

Earlier multi-objective deep learning [Sener and Koltun, 2018, Lin et al., 2019] suffers from increased computational cost with the number of losses, explicit

computation of the gradient with respect to each loss term and gradient norms, making it practically infeasible Mahapatra and Rajan [2021] for large neural networks and large datasets. For instance, Pareto Invariance Risk Minimization (PAIR) [Chen et al., 2022b] studies domain generalization with the use of the multi-objective optimization technique Exact Pareto Optimal Search (EPOS) [Mahapatra and Rajan, 2021], which requires explicit full gradient information for each loss term and computation of the C matrix with complexity m^2n [Mahapatra and Rajan, 2021]. With m being the number of loss terms (equivalent to $d + 1$ in our paper), and n the dimension of gradient, which is super high in modern neural networks (e.g. 200 million for ResNet50), thus results in heavy memory requirements and excessive computation burden, and hinders the deployment to large-scale networks Chen et al. [2022b]. In comparison, our multi-objective optimization method (M-HOF-Opt) need only d scalar multiplications, thus the extra computation is negligible and can be used in large-scale neural networks. EPOS [Mahapatra and Rajan, 2021] also requires the user to provide a preference vector which can be difficult to set, say with 6 objectives for our case. In addition, Chen et al. [2022b] reported hyperparameter tuning for the preference vector and step length is needed for the method to work properly. In comparison, our method, M-HOF-Opt is preference vector free. It ensures the Pareto descent due to the update rule of our setpoint. There is no requirement to search for step length.

Note that the EPOS method Mahapatra and Rajan [2021] is searching for Exact Pareto optimal [Mahapatra and Rajan, 2021], which might not exist. Chen et al. [2022b] divides the training into two phases where the first phase uses single-objective optimization favoring ERM loss while the second phase is for balancing different loss terms. However, how many computation resources should one set for the first phase is not clear. Furthermore, the first stage (phase) can affect the exact Pareto optimality.

5 EXPERIMENTS

5.1 EXPERIMENTAL SETTING

This section presents our experiments training the domain generalization model DIVA [Ilse et al., 2020] with 6 loss terms defined in Equation (4) on the widely used domain generalization benchmark dataset PACS [Li et al., 2017] with different training schemes. Due to the excessive memory requirements and heavy computation of earlier multi-objective deep learning methods discussed in Section 4, which hinders their appli-

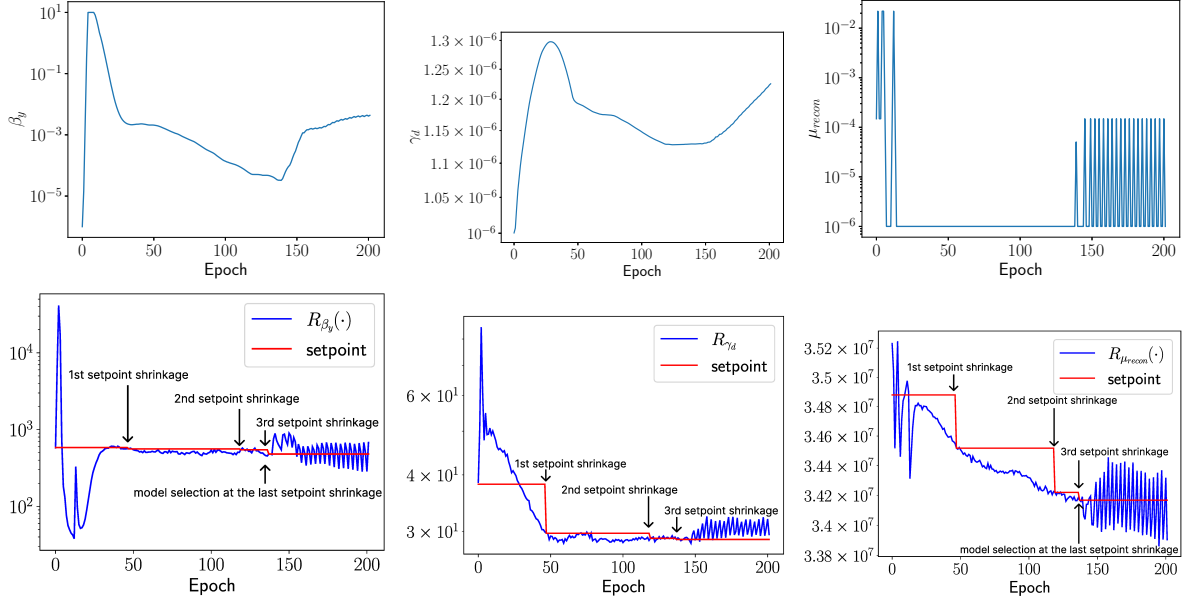


Figure 5: Our method drives the different components of $R(\cdot)$ loss terms down at different scales and rates towards the setpoint, which further promotes the setpoint shrinkage. In the **Top row**, we show the multiplier dynamic as controller output signal in Equation (48) with respect to training epochs. In the **Bottom row**, we present the tracking behavior of the corresponding regularization loss $R(\cdot)$ in Equation (4) with respect to setpoint b defined in Equation (23). This figure is from training DIVA [Ilse et al., 2020] with our multi-objective hierarchical feedback optimization scheme on the PACS dataset [Li et al., 2017]. **Left column**: For the regularization loss of negative KL-divergence corresponding to multiplier β_y in Equation (8) with $R_{\beta_y} = -KL(q_{\phi_y}(z_y|x)||p_{\theta_y}(z_y|y))$ (blue curve), we see that with the setpoint (red curve) initially set to $\rho = 0.99$ in Equation (21) of the initial R_{β_y} value, in the first few epochs R_{β_y} overshoots to an even worse value, but our controller pulls it back towards the setpoint in later epochs via increase in β_y (top figure in the same column) thus adding more weight on $R_{\beta_y}(\cdot)$ in the penalized loss. When R_{β_y} is controlled to be bounded by its setpoint, the corresponding multiplier value β_y also decays to give space for other objectives to decrease (top figure in the same column). With coordinated μ dynamic from each component of the controller output, the setpoint shrinks when all $R(\cdot)$ components Pareto dominates the setpoint. After the setpoint shrinks several times, feasibility in Equation (26) becomes harder to maintain and our controller still keeps R_{β_y} oscillating around the setpoint. Our model selection criteria in Section 3.2.4 selects the model at the last occurrence of the setpoint shrinkage, thus the oscillating behavior at the later epochs can be ignored. **Middle column**: For the domain classification loss R_{γ_d} corresponding to multiplier γ_d in Equation (10) (blue curve), we observe a similar behavior, but the setpoint shrinkage is more visible. **Right column**: Although the output component for the loss $R_{\mu_{recon}}$ in Equation (6) oscillates with relatively large amplitude after the last setpoint shrinkage, our model selection criteria at Section 3.2.4 will exclude this oscillating behavior.

cation, we can only compare our training scheme with other multiplier scheduling techniques. Given that the *sketch* domain within the PACS dataset is considered the most inherently challenging, it was chosen as the sole leave-one-out domain to test the performance of domain generalization. We run experiments to answer the following questions:

- Is our multiplier controller capable of adjusting multidimensional multipliers automatically to drive each component of $R(\cdot)$ at different scales to the setpoint? Does the setpoint shrink, which implies multi-objective descent? We answer these

questions with Figure 5 and Figure 6.

- Will wrong multiplier choices for warmup and fixed multiplier training schemes result in catastrophic effects? Although our method in contrast is multiplier-free, it does need multiplier initial condition $\mu^{(0)}$ and controller hyperparameters. Does varying those have detrimental effects on the predicative performance as well? We answer this question with the benchmark setting in Section 5.1.1 and the results presented in Figure 7.

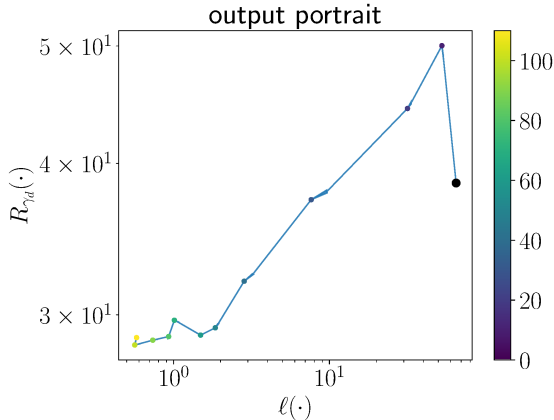


Figure 6: Our training scheme adapts the multi-dimensional multiplier μ , steering the optimization process towards a configuration that balances the trade-off between minimizing output $\ell(\cdot) = \mathbb{E}_{q_{\phi_y}(z_y|x)}[\log q_{\omega_y}(y|z_y)]$ in Equation (5) and output $R_{\gamma_d}(\cdot) = \mathbb{E}_{q_{\phi_d}(z_d|x)}[\log q_{\omega_d}(d|z_d)]$ in Equation (10). In this plot, the solid large point corresponds to the initial output. We use gradually changing colors to indicate the training iterations (epochs), indicated by the color bar. For improved visualization, we exclusively utilized the initial 120 epochs and plotted data points solely for every 10 epochs. This figure corresponds to Figure 5.

5.1.1 Benchmark setting

In the benchmark, we sample different combinations of hyperparameters, (including multiplier for baselines and controller hyperparameter for our method) for each method to be compared. For baselines, we sample $\gamma_d \in \{1, 1001, 100001\}$ and $\gamma_y \in \{1, 1001, 100001\}$ value combinations, and set the ultimate values of β_y, β_d to be 1.0, following [Ilse et al., 2020]. Our method does not need to set ultimate values for μ , so we sample controller hyperparameters, as well as different initial conditions $\mu^{(0)}$ (Each component of the $\mu^{(0)}$ vector set to be the same value).

5.2 RESULTS AND DISCUSSION

Regarding the dynamics of how the setpoint b decreases: Initially, Equation (27) holds, in which case we do not update the setpoint, even if some but not all the blue curves (corresponding to $R(\cdot)$ components) are below the red curves (components of the setpoint). After all constraints for each component of $R(\cdot)$ are satisfied as described in Equation (26), the setpoint (red curves) also gets adapted to a new value (which we term shrinkage), as a new goal to be reached by the $R(\cdot)$ loss in Equation (10). Note that the shrink-

age of setpoint depends on Pareto dominance in Equation (24a), while non-dominance defined an equivalent relation in Definition 2.2. Our hierarchical output feedback optimization training scheme produced the dynamics of $R(\cdot)$ shown in Figure 5 together with the corresponding setpoints b and multipliers. Note that the multiplier $\beta_y, \gamma_d, \mu_{recon}$ and their corresponding loss components operate at different numerical ranges, but our controller still manages to drive the different $R(\cdot)$ loss terms down at different scales and rates.

Figure 6 shows the output portrait of $\ell(\cdot)$ versus a component of $R(\cdot)$ of our training scheme in correspondence to Figure 5. With the multi-objective setpoint based model selection criteria in Section 3.2.4, our method admits a multi-objective descent of the selected model compared to the initial output, such that the uncontrolled behavior at the end of iterations can be safely ignored.

From Figure 7, we can observe that the generalization performance of baselines is highly sensitive to hyperparameter selection. In contrast, our method, as supported by the adaptive behaviors visualized in Figure 5, automatically adjusts the multipliers during the training process, leading to a more robust performance with respect to changes of controller hyperparameters and multiplier initial condition $\mu^{(0)}$. Our method does not need hyperparameter searching of the multiplier, thus saves a fair amount of computational resources.

6 CONCLUSION

This work addresses the issue of combinatorial choice for multidimensional multipliers weighting many terms in neural network loss function. We proposed a probabilistic graphical model for joint multiplier and model parameter optimization with respect to a multi-objective descent of all loss terms. The estimation of model parameter leads to an automatic adjustment scheme for the multipliers, adopting a hierarchical control scheme, which breaks the multi-objective optimization problem into a series of constraint optimization sub-problems. Each sub-problem is configured with a self-adaptive multi-objective setpoint updated via Pareto dominance. A PI-like multiplier controller drives the loss term to satisfy the setpoint constraint for each sub-problem. Our method operates at the timescale of epoch level during training, thus circumvents the need for exhaustive multiplier search and saves tremendous computational resources compared to methods like Bayesian optimization. It also circumvents the excessive memory requirements and heavy computational burden of existing multi-objective deep learning methods. Our method demonstrates robust generalization performance in the PACS domain gen-

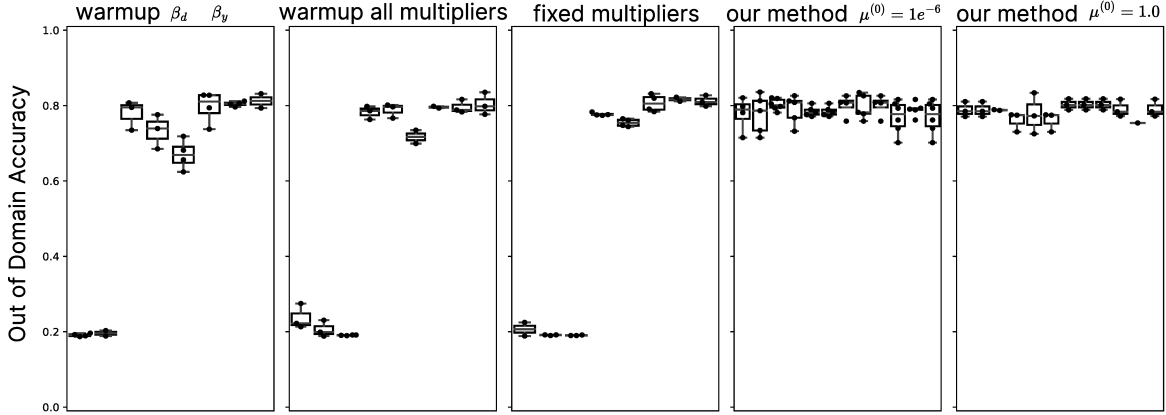


Figure 7: Our automatic multiplier adjustment scheme ensures robust out-of-domain test accuracy when training DIVA [Ilse et al., 2020] with the modified *ResNet50* from [Gulrajani and Lopez-Paz, 2020] on PACS dataset (testing on domain *sketch* and training on domain *photo*, *art-painting* and *cartoon*). Each panel (i.e., subplot) corresponds to a training scheme. Each box plot inside a panel corresponds to a specific hyperparameter (e.g. multiplier value or controller hyperparameters) combination. Inside each box plot, we repeat the experiment with different random seeds corresponding to the dots scatter. In the first panel, we warm up only β_y , β_d in Equations (8) and (9) to their ultimate value 1 while sampling fixed multiplier γ_d and γ_y while fixing $\mu_{recon} = 1.0$. In the second panel, additionally, we also warm up μ_{recon} in Equation (6) to 1.0 and warm up γ_d in Equation (10) to the sampled value, and keep γ_y fixed to be the sampled value. In the third panel, we use fixed constant multipliers without warm-up while keep $\beta = 1$ and $\mu_{recon} = 1$ and only sample γ_d, γ_y combinations. The last two panels correspond to results utilizing our multi-objective hierarchical feedback optimization training method, and we let μ include all multipliers except $\gamma_y = 1$ in Equation (5). For simplicity, when we write $\mu^{(0)} = 1.0$ where $\mu^{(0)} \in \mathbb{R}_+^d$, we mean each component of $\mu^{(0)}$ equals 1.0.

eralization task with Domain Invariant Variational Autoencoding Ilse et al. [2020], compared to other multiplier choice or scheduling schemes which produce very unstable behavior in the training due to the need for a combinatorial choice of multipliers. Our method is multiplier-free since the multiplier is the output of our controller, and it has robust performance with respect to different multiplier initial values. For future work, we are interested in testing the performance of our hierarchical feedback optimization on other domain generalization methods, as well as on other deep learning fields in the form of Equation (1). Theoretically, it is interesting to validate Conjecture 3.1, derive sufficient conditions, incorporate more mathematical analysis into multidimensional case for R , and investigate the potential μ convergence behavior.

7 CONTRIBUTIONS AND ACKNOWLEDGEMENT

XS proposed the idea, developed the theories and algorithms, implemented the code, designed and carried out the experiments, processed experimental data and generated the figures, wrote the manuscript. NC

proposed the PI-like multiplier adaptation in Section 3.2.3, helped XS with PI-like controller implementation, held various discussions, proofread and improved the manuscript. AG initiated the visualization code for Figure 5 and Figure 6, refined by XS, proofread and improved the manuscript. YX developed Corollary 3.2 and corresponding remarks with XS, proofread and improved the constraint optimization part of the theory, discussed on control theory part. CF initiated the benchmark code with refinements from XS, proofread Corollary 3.1. ED and FD tested and improved the code for benchmark, proofread the manuscript. FD further improved the *tensorboard* visualization of the algorithm. LB proofread Corollary 3.1, tested the benchmark code. DS tested the benchmark code, assisted XS in collecting experimental results. CM supervised the project, offered intensive and in depth proofreads of the manuscript with major quality improvements.

We sincerely thank Dr. Changxin Liu and Dr. Prof. Jann Rolfes for spending hours on proofreading the manuscript and offering many helpful suggestions to the manuscript. We thank Tomas Chobola for *Inkscape* support. We thank the anonymous reviewers for offer-

ing suggestions to enhance the readability of our paper.

REFERENCES

- Mokhtar S Bazaraa, Hanif D Sherali, and Chitharanjan M Shetty. *Nonlinear programming: theory and algorithms*. John Wiley & sons, 2013.
- Dimitri P Bertsekas. *Constrained optimization and Lagrange multiplier methods*. Academic press, 2014.
- Fabio M Carlucci, Antonio D’Innocente, Silvia Bucci, Barbara Caputo, and Tatiana Tommasi. Domain generalization by solving jigsaw puzzles. In *Proceedings of the IEEE/CVF Conference on Computer Vision and Pattern Recognition*, pages 2229–2238, 2019.
- Nutan Chen, Patrick van der Smagt, and Botond Cseke. Local distance preserving auto-encoders using continuous knn graphs. In *Topological, Algebraic and Geometric Learning Workshops 2022*, pages 55–66, 2022a.
- Xi Chen, Yan Duan, Rein Houthoofd, John Schulman, Ilya Sutskever, and Pieter Abbeel. Infogan: Interpretable representation learning by information maximizing generative adversarial nets. In *Advances in neural information processing systems*, pages 2172–2180, 2016.
- Yongqiang Chen, Kaiwen Zhou, Yatao Bian, Binghui Xie, Bingzhe Wu, Yonggang Zhang, Kaili Ma, Han Yang, Peilin Zhao, Bo Han, et al. Pareto invariant risk minimization: Towards mitigating the optimization dilemma in out-of-distribution generalization. *arXiv preprint arXiv:2206.07766*, 2022b.
- Thomas G Dietterich et al. The maxq method for hierarchical reinforcement learning. In *ICML*, volume 98, pages 118–126, 1998.
- John C Doyle, Bruce A Francis, and Allen R Tannenbaum. *Feedback control theory*. Courier Corporation, 2013.
- Yaroslav Ganin, Evgeniya Ustinova, Hana Ajakan, Pascal Germain, Hugo Larochelle, François Laviolette, Mario Marchand, and Victor Lempitsky. Domain-adversarial training of neural networks. *The journal of machine learning research*, 17(1):2096–2030, 2016.
- Roman Garnett. *Bayesian optimization*. Cambridge University Press, 2023.
- Andreia P Guerreiro, Carlos M Fonseca, and Luís Paquete. The hypervolume indicator: Computational problems and algorithms. *ACM Computing Surveys (CSUR)*, 54(6):1–42, 2021.
- Ishaan Gulrajani and David Lopez-Paz. In search of lost domain generalization. *arXiv preprint arXiv:2007.01434*, 2020.
- Adrian Hauswirth, Zhiyu He, Saverio Bolognani, Gabriela Hug, and Florian Dörfler. Optimization algorithms as robust feedback controllers. *Annual Reviews in Control*, 57:100941, 2024.
- Zhiyu He, Saverio Bolognani, Jianping He, Florian Dörfler, and Xinping Guan. Model-free nonlinear feedback optimization. *IEEE Transactions on Automatic Control*, 2023.
- Frank Hutter, Holger H Hoos, and Thomas Stützle. Automatic algorithm configuration based on local search. In *Aaai*, volume 7, pages 1152–1157, 2007.
- Frank Hutter, Manuel López-Ibáñez, Chris Fawcett, Marius Lindauer, Holger H Hoos, Kevin Leyton-Brown, and Thomas Stützle. Aclib: A benchmark library for algorithm configuration. In *Learning and Intelligent Optimization: 8th International Conference, Lion 8, Gainesville, FL, USA, February 16-21, 2014. Revised Selected Papers 8*, pages 36–40. Springer, 2014.
- Maximilian Ilse, Jakub M Tomczak, Christos Louizos, and Max Welling. Diva: Domain invariant variational autoencoders. In *Medical Imaging with Deep Learning*, pages 322–348. PMLR, 2020.
- Michael A Johnson and Mohammad H Moradi. *PID control*. Springer, 2005.
- Diederik P Kingma and Jimmy Ba. Adam: A method for stochastic optimization. *International Conference for Learning Representations*, 2015.
- A. Klushyn, N. Chen, R. Kurle, B. Cseke, and P. van der Smagt. Learning hierarchical priors in VAEs. *Advances in Neural Information processing Systems*, 32, 2019.
- Daphne Koller and Nir Friedman. *Probabilistic graphical models: principles and techniques*. MIT press, 2009.
- Tejas D Kulkarni, Karthik Narasimhan, Ardavan Saeedi, and Josh Tenenbaum. Hierarchical deep reinforcement learning: Integrating temporal abstraction and intrinsic motivation. *Advances in neural information processing systems*, 29, 2016.
- Matan Levi, Idan Attias, and Aryeh Kontorovich. Domain invariant adversarial learning. *arXiv preprint arXiv:2104.00322*, 2021.
- Sergey Levine. Reinforcement learning and control as probabilistic inference: Tutorial and review. *arXiv preprint arXiv:1805.00909*, 2018.
- Frank L Lewis, Draguna Vrabie, and Vassilis L Syrmos. *Optimal control*. John Wiley & Sons, 2012.
- Da Li, Yongxin Yang, Yi-Zhe Song, and Timothy M Hospedales. Deeper, broader and artier domain generalization. In *Proceedings of the IEEE international conference on computer vision*, pages 5542–5550, 2017.
- Da Li, Yongxin Yang, Yi-Zhe Song, and Timothy M Hospedales. Learning to generalize: Meta-learning for domain generalization. In *Proceedings of the AAAI conference on artificial intelligence*, volume 32, 2018.
- Xi Lin, Hui-Ling Zhen, Zhenhua Li, Qing-Fu Zhang, and Sam Kwong. Pareto multi-task learning. *Advances in neural information processing systems*, 32, 2019.

- Manuel López-Ibáñez, Jérémie Dubois-Lacoste, Leslie Pérez Cáceres, Mauro Birattari, and Thomas Stützle. The irace package: Iterated racing for automatic algorithm configuration. *Operations Research Perspectives*, 3:43–58, 2016.
- Debabrata Mahapatra and Vaibhav Rajan. Exact pareto optimal search for multi-task learning: Touring the pareto front. *arXiv e-prints*, pages arXiv–2108, 2021.
- Tristan Milne. Piecewise strong convexity of neural networks. *Advances in Neural Information Processing Systems*, 32, 2019.
- Miguel Picallo, Saverio Bolognani, and Florian Dörfler. Closing the loop: Dynamic state estimation and feedback optimization of power grids. *Electric Power Systems Research*, 189:106753, 2020.
- Philipp Probst, Anne-Laure Boulesteix, and Bernd Bischl. Tunability: Importance of hyperparameters of machine learning algorithms. *The Journal of Machine Learning Research*, 20(1):1934–1965, 2019.
- Alexandre Rame, Corentin Dancette, and Matthieu Cord. Fishr: Invariant gradient variances for out-of-distribution generalization. In *International Conference on Machine Learning*, pages 18347–18377. PMLR, 2022.
- Sashank J Reddi, Satyen Kale, and Sanjiv Kumar. On the convergence of adam and beyond. *arXiv preprint arXiv:1904.09237*, 2019.
- D. J. Rezende and F. Viola. Taming VAEs. *CoRR*, 2018.
- Ozan Sener and Vladlen Koltun. Multi-task learning as multi-objective optimization. *Advances in neural information processing systems*, 31, 2018.
- Huajie Shao, Shuochao Yao, Dachun Sun, Aston Zhang, Shengzhong Liu, Dongxin Liu, Jun Wang, and Tarek Abdelzaher. Controlvae: Controllable variational autoencoder. In *International Conference on Machine Learning*, pages 8655–8664. PMLR, 2020.
- Anthony Sicilia, Xingchen Zhao, and Seong Jae Hwang. Domain adversarial neural networks for domain generalization: When it works and how to improve. *Machine Learning*, pages 1–37, 2023.
- Casper Kaae Sønderby, Tapani Raiko, Lars Maaløe, Søren Kaae Sønderby, and Ole Winther. Ladder variational autoencoders. *Advances in neural information processing systems*, 29, 2016.
- Xudong Sun and Bernd Bischl. Tutorial and survey on probabilistic graphical model and variational inference in deep reinforcement learning. In *2019 IEEE Symposium Series on Computational Intelligence (SSCI)*, number 1908.09381, 2019.
- Xudong Sun and Florian Buettner. Hierarchical variational auto-encoding for unsupervised domain generalization. *ICLR 2021 RobustML*, *arXiv preprint arXiv:2101.09436*, 2021.
- Xudong Sun, Andrea Bommert, Florian Pfisterer, Jörg Rahnenführer, Michel Lang, and Bernd Bischl. High dimensional restrictive federated model selection with multi-objective bayesian optimization over shifted distributions. *arXiv preprint arXiv:1902.08999*, 2019a.
- Xudong Sun, Alexej Gossmann, Yu Wang, and Bernd Bischl. Variational resampling based assessment of deep neural networks under distribution shift. In *2019 IEEE Symposium Series on Computational Intelligence (SSCI)*, number 1906.02972, 2019b.
- Xudong Sun, Jiali Lin, and Bernd Bischl. Reinbo: Machine learning pipeline conditional hierarchy search and configuration with bayesian optimization embedded reinforcement learning. In *Machine Learning and Knowledge Discovery in Databases: International Workshops of ECML PKDD 2019, Würzburg, Germany, September 16–20, 2019, Proceedings, Part I*, pages 68–84. Springer International Publishing, 2020.
- Eckart Zitzler and Simon Künzli. Indicator-based selection in multiobjective search. In *International conference on parallel problem solving from nature*, pages 832–842. Springer, 2004.
- Eckart Zitzler, Dimo Brockhoff, and Lothar Thiele. The hypervolume indicator revisited: On the design of pareto-compliant indicators via weighted integration. In *Evolutionary Multi-Criterion Optimization: 4th International Conference, EMO 2007, Matsushima, Japan, March 5-8, 2007. Proceedings 4*, pages 862–876. Springer, 2007.